Ocean Dynamics (2026) 76:30
https://doi.org/10.1007/s10236-026-01786-8

Wave climate variability along the selected erosional hotspots of Kerala

Prince Arayakandy[2] · P G Remya[1] · Meenakshi Sreejith[1] · Phiros Shah[3] · Ratheesh Ramakrishnan[4] · B Praveen Kumar[1] · Alfred Johny[5] · T M Balakrishnan Nair[1]

Received: 22 September 2025 / Accepted: 22 February 2026

Abstract
Coastal regions across the globe are increasingly threatened by erosion and inundation as rising sea levels and shifting wave climates intensify these hazards. Within this global context, the state of Kerala on the southwestern coast of India stands out as particularly vulnerable due to its high population density and extensive coastal exposure. The present study analyses the wave climate variability over the recent 15-year period (2007–2021) across 19 coastal sites in Kerala that are recognized as hotspots for erosion and inundation. Using the WAVEWATCH III model output, annual and monthly trends in the mean and near-extreme (90th percentile) significant wave height (SWH), swell wave height (SHTS) and wind sea wave height (SHWW) were analysed. The model data is validated with available buoy data at six locations (both east and west coast) along the Indian coastline. Results reveal a coherent intensification of wave conditions, with most locations exhibiting statistically significant positive trends. Musodi beach in Kasargod, the northernmost site, exhibited the highest trend in annual mean SWH, with an increase of 0.863 cm/year. Monthly trend analysis revealed a significant positive trend in the SWH, SHTS and SHWW during May and August months especially in the northern locations. Spatial trend analysis of SWH, SHTS, and SHWW highlighted a significant upward trend in the Southern Ocean during May and August, establishing the strong teleconnection. The combined rise in SWH, SHTS, and SHWW underscores an ongoing intensification of nearshore wave energy, with important implications for shoreline change, sediment dynamics, and hazard risk. These findings underscore the need for advanced coastal management strategies, integrating long-term wave climate monitoring and mitigation measures to reduce coastal hazards along the coast of Kerala.

Keywords Erosion · Wave climate · WAVEWATCH III · Significant wave height · Indian Ocean

1 Introduction

Coastal communities across the globe are threatened by the dual challenges of coastal erosion and inundation, problems that are expected to be aggravated due to rising sea levels (Beaven et al. 2020). These complex processes are influenced by a variety of natural and human-induced factors, and these factors exhibit variability across different coastal regions (Almar et al. 2015). Among these factors, wave climate variability stands out as one of the major components that are responsible for coastal inundation and erosion. Several coastlines have been reported to experience high wave energy and increased longshore current, which worsens coastal erosion (Sreelakshmi and Bhaskaran 2023). Therefore, understanding the wave climate variability is essential to carry out coastal protection works, as well as for effective

Responsible Editor: Prasad Bhaskaran

✉ P G Remya
remya.pg@incois.gov.in

[1] MoES-Indian National Centre for Ocean Information Services, Hyderabad, India

[2] Faculty of Fisheries Engineering, Kerala University of Fisheries and Ocean Studies, Kochi, Kerala, India

[3] Kerala University of Fisheries and Ocean Studies, Kochi, Kerala, India

[4] Space Applications Centre (ISRO), Ahmedabad, India

[5] College of Climate Change and Environmental Science, Kerala Agricultural University, Kerala, India

Published online: 11 March 2026

marine renewable energy exploitation, ship routing, and the prediction/warning of extreme events.

Wave climate studies across the globe have been carried out using model products, satellite altimetry, buoy data, and ship-based observations. Using satellite-based altimeter measurements spanning 23 years from 1985 to 2008, Young et al. (2011) revealed an increasing trend of 0.25% and 0.50% per year for extreme (90th and 99th, respectively) SWH in both hemispheres. Between 1980 and 2014, 30–40% of the world's oceans experienced significant seasonal trends in mean and extreme wave height, period, and direction. The Southern hemisphere in particular exhibited strong positive trends in wave heights, with trends of 1–2 cm per year (Erikson et al. 2022).

Building on such global-scale trends, numerous regional studies have analysed the wave climate variability in specific basins, including the North Atlantic, Pacific, Indian and Southern Oceans, to understand localised trends and driving mechanisms (Li et al. 2018; Kumar et al. 2019; Lemos et al. 2021). The regional assessments are crucial for planning and protection of vulnerable coasts around the globe. This aspect is very important for the Indian Ocean, where wave characteristics are strongly modulated by monsoonal winds and swell propagation from the Southern Ocean, and hence, detailed regional analyses have gained momentum in recent years. Sreelakshmi and Bhaskaran (2020a, b, c) conducted detailed studies on the wind and wave climatology in the Indian Ocean using global datasets ERA-Interim, ERA40, and ERA5. The impact of Southern Ocean swells in the NIO and Indian coastal areas are addressed in many studies (Sabique et al. 2012; Remya et al. 2016).

These regional wave climate studies highlight the importance of coastal studies, particularly in vulnerable coastal areas like the North Indian Ocean (NIO). The wave climatology of the NIO is particularly unique due to the seasonal reversal of wind during the two seasons, the southwest monsoon (SWM) and the northeast monsoon (NEM). Moreover, the NIO wave climate is strongly influenced by the swells propagating from the Southern Ocean especially during June to September (Young 1999). Southern Ocean swells and the swell wave field resulting from northwest (NW) winds in the Arabian Sea (Shamal and Makran swells) also influence the NIO (Sreelakshmi and Bhaskaran (2020c). These swells alter and modulate the local wind-wave conditions during their propagation towards the coast.

Within the NIO, the state of Kerala, located along the southwestern coast of India, is particularly vulnerable to coastal hazards due to its high population density and significant coastal exposure. Erosion during the monsoon season and following beach buildup during the post monsoon period have been studied for some locations along the coast (Kurian 1988; Thomas 1988; Shahul Hameed 1988, 2007; Harish 1988). Previous studies describe the spatial variations in the nearshore wave intensity and related coastal processes along the coast (Kurian et al. 2009). Chowdhury et al. (2019) projected an upcoming increase of around 0.1 m for significant wave height (SWH) and 0.8 m for maximum wave height (Hmax) along the Kerala coast. Additionally, they anticipated a moderate (5%) increase in mean wave period and clustering of waves predominantly from the southwest direction compared to the current climate. These projected wave conditions can influence coastal processes, coastal ecosystems, and sediment transport rates, causing erosion/accretion, hence making the coast more vulnerable to the impact of climate change. The Kerala coast also encounters kallakkadal flash flooding events associated with the swells generated by cut-off low systems in the Southern Indian Ocean (SIO) (Remya et al. 2016). During the tropical cyclone Tauktae in May 2021, infragravity waves and wave setup significantly contributed to the overtopping of waves and severe coastal inundation at Chellanam in Ernakulam district of Kerala (Ramakrishnan et al. 2022). Recently, Ananthu et al. (2026), utilising 83 years of ERA5 reanalysis wave data evaluated the interannual and decadal variations in significant wave height, focusing on mean, 90th percentile and maximum values along the 10 coastal locations of Kerala. They concluded that significant wave height has exhibited notable temporal variability, with certain locations showing increasing trends, likely influenced by large-scale climatic drivers and regional oceanographic conditions.

While numerous studies have been conducted on wave climate variability along global and regional scales (Shanas and Sanil Kumar 2014; SanilKumar and Jesbin 2016; Naseef and Kumar 2017; Saprykina et al., 2021 etc.), there is no study reported so far that investigated the wave climate change exclusively for erosional/inundation hotspots along the Kerala coast. Hence, we have examined the annual/monthly trend in the mean and near-extreme (90th percentile) estimated significant wave height (SWH), significant wave height of total swell (SHTS) and the significant wave height of wind sea (SHWW) along the selected erosional hotspots of Kerala.

The manuscript is organized as follows. Section 2 discusses the datasets used and the methodology followed. Section 3 details the major results of this study. Section 4 discusses the major conclusion, possible limitations, and future scope of the study.

2 Data and methods

2.1 Study locations

The Kerala coast, located on the southwest coast of India, comprises 9 coastal districts and shares its coastal boundary with the Arabian Sea. The 593 km-spanning coast comprises sandy beaches, estuaries, bays, lagoons, rocky cliffs, headlands, sand dunes, barriers, spits, tombolos, etc. The southern Kerala coast is characterised by high energy levels, coarse sediments and a steep inner shelf. In contrast, the central and northern Kerala coasts exhibit a moderate energy regime, featuring a gentle inner shelf covered with fine sediments, unique for the occurrence of mudbanks at different locations (Noujas et al. 2019). The strong southwest monsoon severely impacts the coastal belt of Kerala (Shamji et al. 2010).

Nineteen erosional/inundation hotspot locations are selected through a comprehensive literature review and on field visits along the Kerala coast (Shoreline change atlas of the Indian Coast (Volume 3)). Figure 1; Table 1 present the selected study locations.

2.2 Model setup

Wave fields for the study were generated using WAVEWATCH III (WW3), version 6.07 (Tolman and the WAVEWATCH III Development Group, 2019), incorporating the parameterization scheme ST4 by Ardhuin et al. 2010. The INCOIS-WW3 setup used for the present study has three mosaic grids in a nested pattern (Global [0°–360°, 80° S–80°N], Indian Ocean [30°E–120°E, 60°S–30°N], and North Indian Ocean [45°-100°E, 0°-25°N]) with spatial resolutions of 0.5°, 0.125°, and 0.05°, respectively. ETOPO1 bathymetry (1′ arc length global relief bathymetry dataset) from the National Geophysical Data Centre and the global shoreline database (GSHHS—Global Self-Consistent Hierarchical High-Resolution Shoreline) is used with an automated grid generation package V2.219 based on an algorithm designed to meld the high-resolution bathymetry with the shoreline database to develop the optimum grid (Chawla et al. 2007). The wave model is configured for a spectral frequency ranging from 0.035 to 0.5 Hz (29 frequencies) with a gradual increment of 10%, and the spectral direction is discretised into 36 portions. Wave fields were

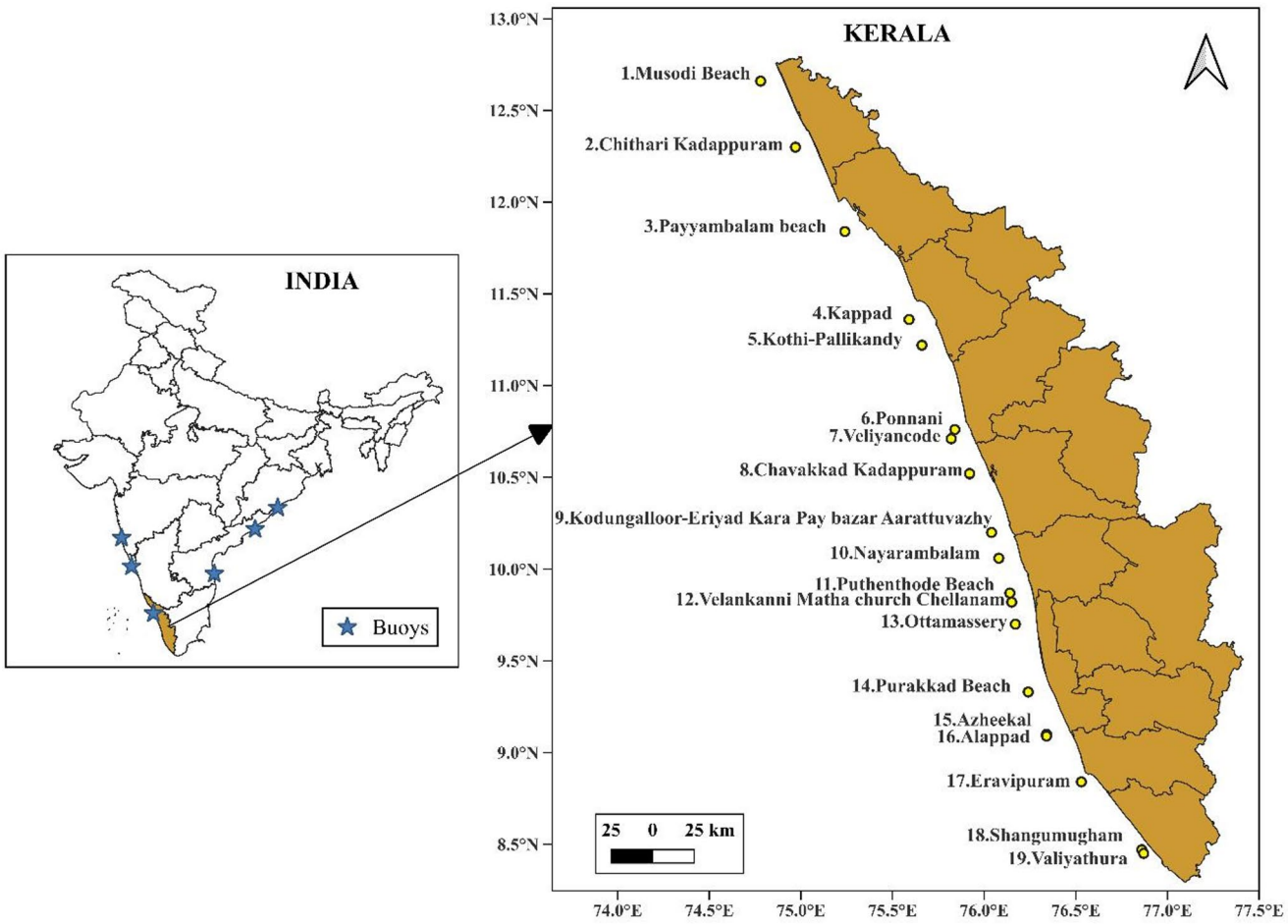

Fig. 1 Locations of buoys used for validation and 19 selected locations along the Kerala coast

Table 1 Selected locations with geo-coordinates

Sl No.	Location, district	Geo-Coordinates	Depth (m)
1	Musodi Beach, Kasargod	12.66 N, 74.78E	26
2	Chithari Kadappuram, Kasargod	12.3 N, 74.97E	24
3	Payyambalam Beach, Kannur	11.84 N, 75.24E	24
4	Kappad, Kozhikode	11.36 N, 75.59E	24
5	Kothi-Pallikandy, Kozhikode	11.22 N, 75.66E	22
6	Ponnani, Malappuram	10.76 N, 75.84E	19
7	Veliyancode Malappuram	10.71 N, 75.82E	25
8	Chavakkad-Kadappuram, Thrissur	10.52 N, 75.92E	22
9	Kodungalloor-Eriyad, Kara, Pay bazar, Aarattuvazhy, Thrissur	10.2 N, 76.04E	22
10	Nayarambalam, Thrissur	10.06 N, 76.08E	22
11	Puthenthode beach, Ernakulam	9.87 N, 76.14E	22
12	Velankanni Matha church Chellanam, Ernakulam	9.82 N, 76.15E	23
13	Ottamassery, Alappuzha	9.7 N, 76.17E	23
14	Purakkad beach, Alappuzha	9.33 N, 76.24E	26
15	Azheekal, Kollam	9.1 N, 76.34E	26
16	Alappad, Kollam	9.09 N, 76.34E	30
17	Eravipuram, Kollam	8.84 N, 76.53E	28
18	Shangumugham, Trivandrum	8.47 N, 76.86E	31
19	Valiyathura, Trivandrum	8.45 N, 76.87E	37

generated for a period of 15 years from 2007 to 2021. The model results of significant wave height (SWH/Hs), swell wave height (SHTS), wind-sea height (SHWW), mean wave direction (MWD) and wind speed (Ws) has been used to complete this study.

2.3 ERA5 reanalysis

This study used the European Centre for Medium-Range Weather Forecast (ECMWF) Reanalysis v5 (ERA5; Hersbach et al. 2020) data with spatial resolution of $0.5^0 \times 0.5^0$ for wave parameters. ERA5 data for a period of 15 years from 2007 to 2021 was used for cross-referencing trends results with WW3 trends. The wave parameters used are SWH, SHWW and SHTS.

2.4 Model validation using in-situ observations

The WW3 model results are validated using data from the WAMAN network, which is managed by the Earth System Science Organization - Indian National Centre for Ocean Information Services (ESSO-INCOIS) (Balakrishnan et al. 2025). The buoy data from six locations (both east and west coast) along the Indian coastline have been used for a three-year period (2020–2022). The directional waverider buoy features a spherical casing with a diameter of 0.9 m, containing three orthogonally arranged accelerometers: one in the vertical direction and two in the horizontal directions. The vertical and horizontal (eastward and northward) displacements are obtained through double integration of the respective acceleration signals, without applying a filter. The displacement data are continuously recorded at a frequency of 1.28 Hz and processed every 30 min into a single record.

The model error statistics, including bias, root mean square error (RMSE), Scatter Index (SI) and correlation (R), have been done in this study using the following relations:

$$Bias = \sum_{i=1}^{N} \left(\frac{1}{n} (y_i - x_i) \right)$$

$$RMSE = \frac{1}{n} \sqrt{\sum_{i=1}^{N} (y_i - x_i)^2}$$

$$R = \frac{\sum_{i=1}^{N} \left(y_i - \bar{y} \right) \left(x_i - \bar{x} \right)}{\sqrt{\frac{1}{n} \sum_{i=1}^{N} \left(y_i - \bar{y} \right)^2} \sqrt{\frac{1}{n} \sum_{i=1}^{N} \left(x_i - \bar{x} \right)^2}}$$

$$SI = \frac{RMSE}{\bar{x}} \times 100$$

Where, x and y represent buoy and model wave parameters and $\bar{x}$ and $\bar{y}$ represents the mean of the buoy and model results.

The wave model demonstrates strong agreement with wave rider buoy observations across six Indian coastal locations (Table 2). Krishnapatnam shows the best performance with low error (RMSE = 0.15), minimal bias (0.02), and high correlation (R = 0.95). Ratnagiri also performs exceptionally well, with the highest correlation (R = 0.98) and the lowest scatter (SI = 0.13). Overall, the model exhibits reliable accuracy, particularly in Krishnapatnam and Ratnagiri, with minor regional variations in bias and error.

2.5 Trend estimate

The trend is assessed by estimating the slope of the linear best-fit curve to the annual mean / near-extreme (90th percentile) of SWH, SHTS and SHWW over the 15 years

Table 2 Statistics of model validation against Waverider buoy observations along the Indian coastline for three years (2020–2022)

Location/depth	Bias	RMSE	R	SI
Gopalpur (22 m)	-0.02	0.17	0.94	0.16
Visakhapatnam (15 m)	-0.08	0.2	0.93	0.19
Krishnapatnam (19 m)	0.02	0.15	0.95	0.17
Kozhikode (19 m)	0.1	0.21	0.96	0.18
Karwar (15 m)	-0.02	0.23	0.96	0.13
Ratnagiri (18 m)	-0.05	0.18	0.98	0.13

(Young et al. 2011). A positive slope value indicates an upward trend, while a negative slope value indicates a downward trend. Additionally, assessed the monthly linear trends in mean and near-extreme (90th percentile) wave parameters from 2007 to 2021. Statistical analysis was performed, and the significance level was set at 90%, trends with a p-value less than 0.10 were considered statistically significant using the Student's t-test.

3 Results and discussions

3.1 Annual and monthly trends in wind and wave parameters

This section presents the annual and monthly trends of Ws, SWH, SHTS, and SHWW at 19 selected locations along the Kerala coast over a 15-year period (2007–2021). The annual Mean trend values for these four parameters are illustrated in Fig. 2.

A general observation from the analysis is that most locations exhibit increasing trends in wind and wave parameters, indicating a gradual rise in wind speeds and wave heights along the Kerala coast during the study period. The northern region, particularly Payyambalam Beach, Kannur (Location 3), recorded the highest significant increase of 5.4 cm s^{-1} yr^{-1} in annual mean wind speed and 7.4 cm s^{-1} yr^{-1} in annual near extreme wind speed. In contrast, the lowest significant increase in annual near extreme windspeed was observed at Kothi, Kozhikode (Location 5) of 3.03 cm s^{-1} yr^{-1}.Most of the locations exhibited an increasing trend in the range 3 to 7 cm s^{-1} yr^{-1} except at a few locations in the central and southernmost tip of the Kerala coast. A recent study by Abdulla et al. (2022) used a longer period of 41 years from 1979 to 2019 and observed an overall decreasing wind speed trend along the Kerala coast. However, in their study, the decade 2010–2019 displayed contrasting increasing trends between Kochi-Kasargod (1.7–3.9 cm s^{-1} $year^{-1}$) and a decreasing trend from Thiruvananthapuram to Alappuzha. Similarly, the annual and near-extreme wind speed (90th percentile) trends observed in the present study also showed good agreement with the recent past trend reported by Abdulla et al. (2023). All the stations in their study along the Kerala coast exhibited an upward trend in extreme windspeed in the past decade with higher magnitudes at Kochi and Kasargod, similar to the present study.

For the Annual mean SWH trend (Fig. 2b), positive trends were noted at 17 out of 19 locations, with the highest increase at Musodi Beach (Location 1) of 0.863 cm/yr followed by 0.859 cm/yr at Eravipuram (Location 17). A north-to-south decreasing gradient in trend magnitude was apparent, except at Eravipuram, which showed a marked local increase. This highlights a more prominent rise in wave activity in northern Kerala compared to central and southern parts over the past decade. In terms of near extremes (Fig. 3b), positive trends were mainly confined to the northern and southern regions, with the highest value at Location 17 and the lowest at Azheekal (Location 15). The observed trends are consistent with the findings of Ananthu et al. (2026), who used 83 years of wave data along the Kerala coast and reported increasing trends in the mean, 90th percentile, 99th percentile and yearly maximum SWH. They identified the strongest increase at Location 8, located close to Eravipuram (Location 17), followed by Locations 1 and 2 in northern Kerala for near-extreme (90th percentile) SWH. This study also revealed a similar spatial pattern, with Location 17 showing the highest trend, followed by Locations 1 and 2.

When the recent decadal trend magnitudes are compared, the agreement becomes even clearer. Ananthu et al. (2026) reported near-extreme SWH trends exceeding ~ 2 cm yr^{-1} at Locations 7 and 8, with slightly lower but still positive trends at Locations 1 and 2. Consistent with this, the present study shows a trend magnitude of 2.094 cm yr^{-1} at Eravipuram (Location 17), followed by Musodi Beach (Location 1) and Chithari Kadapuram (Location 2), with trends of 1.70 and 1.524 cm yr^{-1}, respectively. The close agreement between the two studies indicates that the 15-year analysis captures the ongoing decadal-scale strengthening of near-extreme wave conditions along the Kerala coast.

Since SWH is influenced by both SHTS and SHWW components, trends in these components were also examined. The annual mean SHTS (Fig. 2c) showed the highest trend at Location 1, aligning with the SWH findings. However, the distribution of SHTS trends was more varied, with no clear gradient. Location 17 again emerged as a notable exception with elevated trend values. Near-extreme SHTS (Fig. 3c) showed significant positive trends in the north and scattered increases elsewhere, with the highest value again at Location 17. These patterns suggest a consistent increase in swell heights at this location.

For SHWW (Fig. 2d), the highest annual mean trend was also observed at Location 1, indicating that both swell and wind-sea components contribute to the increasing SWH at this site. While the overall trend distribution was mixed, most locations exhibited a positive trend, especially in central Kerala, highlighting an increasing role of local wind-driven waves. This has been further supported by the changes observed in the probability distribution plot given in Fig. 4. The analysis clearly shows the increase in the higher wave heights (SWH>2 m) in recent years. In contrast, near-extreme SHWW (Fig. 3d) showed weak or no trends in the north but stronger positive trends in the central and southern regions, particularly at Location 17. The contrast between increasing

Fig. 2 Trends in the annual mean wind speed (cm s^{-1} yr^{-1}) and wave parameters (cm yr^{-1}) at the selected locations along the Kerala coast. Filled symbols indicate statistically significant trends at the 90% confidence level

SHWW and relatively mixed SHTS at central locations suggests a decline in swell activity there, while increasing SHTS in the north—without corresponding increases in SHWW—points to greater swell influence in northern Kerala. Notably, the observed rise in wind-sea extremes in central Kerala did not significantly affect the overall extreme SWH values.

The observed trends are consistent with the findings of Ananthu et al. (2026), who used 83 years of wave data along the Kerala coast and reported increasing trends in the mean, 90th percentile, 99th percentile and yearly maximum SWH. They identified the strongest increase at Location 8, located close to Eravipuram (Location 17), followed by Locations 1 and 2 in northern Kerala for near-extreme (90th percentile) SWH. This study also revealed a similar spatial pattern, with Location 17 showing the highest trend, followed by Locations 1 and 2.

When the recent decadal trend magnitudes are compared, the agreement becomes even clearer. Ananthu et

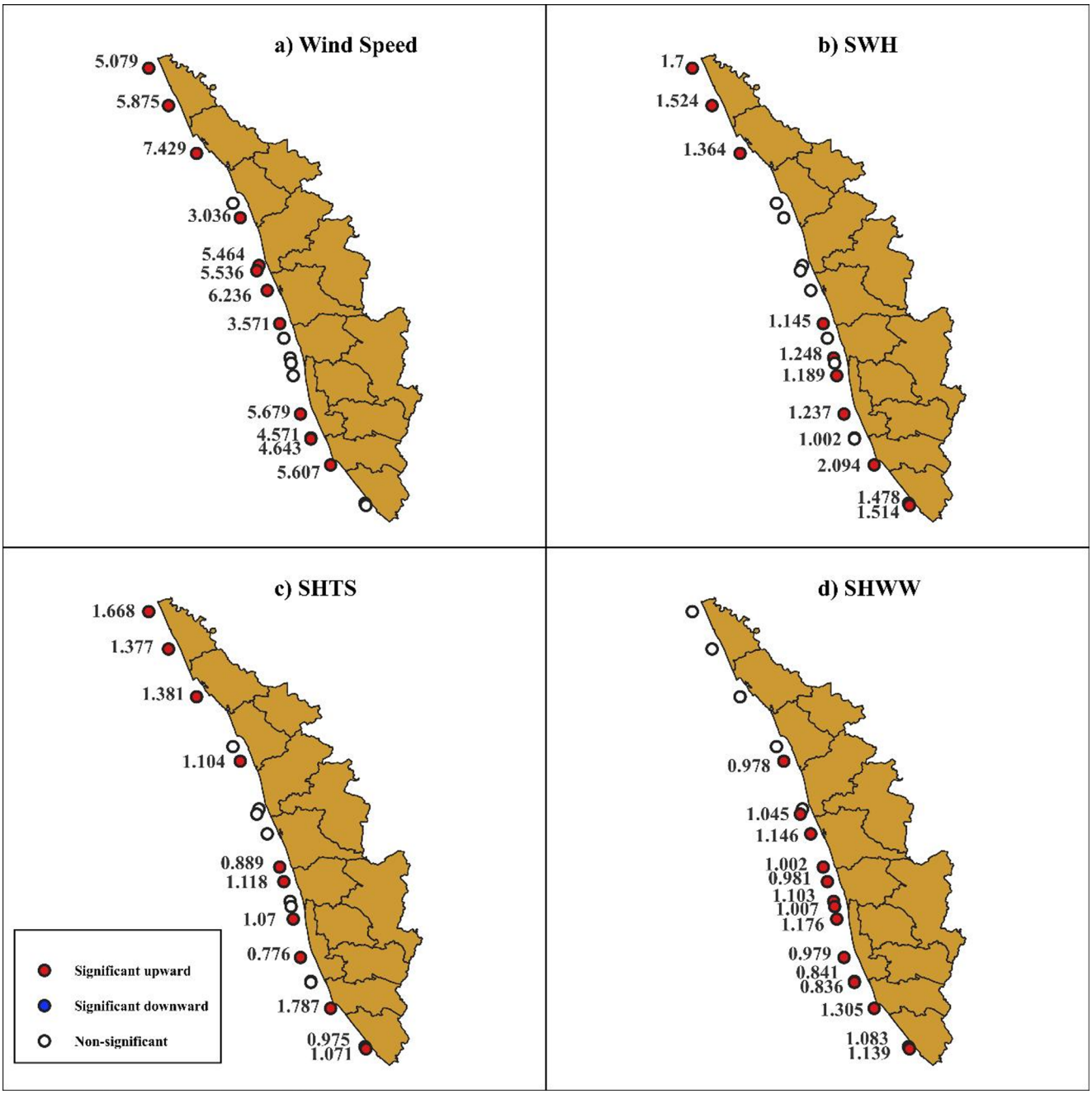

Fig. 3 Trends in the annual near-extreme (90th percentile) wind speed (cm s^{-1} yr^{-1}) and wave parameters (cm yr^{-1}) at the selected locations along the Kerala coast. Filled symbols indicate statistically significant trends at the 90% confidence level

al. (2026) reported near-extreme SWH trends exceeding ~ 2 cm yr^{-1} at Locations 7 and 8, with slightly lower but still positive trends at Locations 1 and 2. Consistent with this, the present study shows a trend magnitude of 2.094 cm yr^{-1} at Eravipuram (Location 17), followed by Musodi Beach (Location 1) and Chithari Kadapuram (Location 2), with trends of 1.70 and 1.524 cm yr^{-1}, respectively. The close agreement between the two studies indicates that the 15-year analysis captures the ongoing decadal-scale strengthening of near-extreme wave conditions along the Kerala coast.

Figure 4 represents the probability density function of SWH at Location 1 for the period of study. Each graph illustrates the distribution of SWH for a given year. The horizontal red dashed line at 2.5 m indicates the rough wave day threshold as a level of interest in identifying extreme wave events (WCRP, 2020). The skewed distribution of significant wave heights is generally consistent across years, with

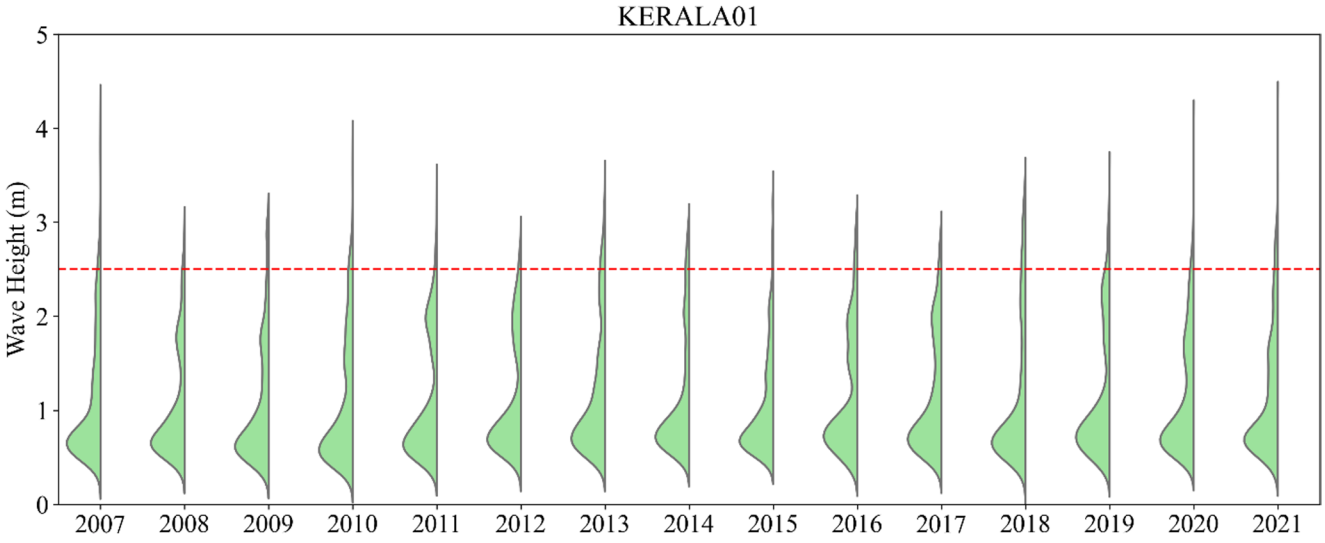

Fig. 4 Probability density function plot showing long-term trends in wave characteristics at location 1

a noticeable peak below 1 m, suggesting a high frequency of relatively calm wave conditions. Additionally, there is a wider, smaller distribution that reaches higher wave heights, indicating the presence of more intense wave events. The violin plots show that while the majority of significant wave heights remain below the 2.5-m threshold, there are tails extending significantly above it in most years. In contrast to other years, years like 2010, 2018, and 2020 seem to show a wider spread towards higher SWH, which may indicate times when high-wave events are more frequent. Years like 2013 and 2015, on the other hand, appear to have a somewhat smaller distribution, indicating fewer instances of extreme wave events. Although there is clear inter-annual variability in the frequency of extreme wave events, the consistent shape of the PDF over time suggests a comparatively stable wave climate.

Analysis of monthly trends for all these parameters is required, as the unique wind reversals in the Indian Ocean contribute to significant changes in wave characteristics along the Indian coastline. The monthly trend analysis of mean and near-extreme Ws is therefore shown in Tables 3 and 4. Mean wind speeds show widespread increases across the majority of locations, with significant positive trends typically ranging from about 3 to 7 cm s^{-1} yr^{-1}. Payyambalam Beach (Location 3) exhibits the highest significant upward trend for most months of the year indicating the exposure of northern Kerala to the alterations in Arabian sea wind forcing. Both tables show overall strengthening of wind speeds across many locations, but the near-extreme winds in Table 4 exhibit larger magnitudes of change compared to the mean winds in Table 3. The strongest increases occur notably in January, February, October, November and December in mean wind speed trends (Table 3). Table 4 near extreme winds shows even more pronounced rises, often exceeding 10 cm s^{-1} yr^{-1} at several sites in these months but the highest increase in near extreme winds is seen during May in most of the locations. Similarly, locations with decreasing / non-significant are consistent between tables (especially Location 10), but the declines are generally more intense in the near-extreme winds. Overall, the comparison indicates that the regional wind climate is not only experiencing increases in average wind speeds but also stronger intensification of near-extreme winds especially in the northernmost locations (1,2,3) of Kerala. In contrast the southernmost locations Shangumugham Beach and Valiyathura Beach (Locations 18 and 19) showed significant downward trends during January of nearly 2 cm s^{-1} yr^{-1} and a much higher decrease during May around 7 cm s^{-1} yr^{-1} in the mean wind speed trends.

The monthly mean SWH trends (Table 5) show a consistent pattern of increasing wave heights across most locations, with statistically significant rises concentrated during the pre-monsoon month of May and the monsoon peak month of August and October. These increases align closely with the strengthening of regional wind forcing shown in earlier wind-speed analyses, particularly in northern and central Kerala. Northern locations (1–9) exhibit strongest mean SWH increases during May (around 1.4–1.9 cm yr^{-1}), reflecting enhanced pre-monsoon wave activity. Similarly, positive trends during August and October associated with active monsoon and post-monsoon conditions, indicate a systematic increase in wave energy across the coastline. Overall, the pattern suggests that both the monsoonal and transitional seasonal wave condition is intensifying.

The near-extreme SWH trends (Table 6) reveal a similar structure but with higher magnitudes and spatial variability, indicating that energetic wave events are becoming stronger more rapidly than mean conditions. As with the mean

Table 3 Mean monthly wind-speed trends (cm s^{-1} yr^{-1}) at the selected locations. Green shading indicates increasing trends, while red shading denotes decreasing trends, significant at 90% confidence level

Location	Jan	Feb	Mar	Apr	May	Jun	Jul	Aug	Sep	Oct	Nov	Dec
01	4.698	-0.243	4.003	0.238	4.757	0.166	1.203	6.435	4.994	5.671	2.491	4.675
02	3.815	0.207	5.657	2.859	5.574	1.089	1.988	6.466	6.272	5.729	3.138	3.990
03	6.068	3.516	6.571	4.292	6.138	2.998	3.370	6.395	9.753	5.552	4.648	6.114
04	1.791	-0.787	1.835	0.652	2.141	0.230	0.690	2.830	6.677	2.537	1.865	3.112
05	2.018	-0.590	2.075	0.740	2.018	1.045	1.712	4.042	7.390	3.002	2.550	3.974
06	5.176	5.516	1.860	1.345	2.409	2.744	3.134	4.561	7.143	3.171	5.586	5.248
07	5.042	5.781	1.764	1.197	2.658	3.178	3.439	5.024	7.447	3.505	6.256	5.587
08	3.645	6.556	1.510	0.722	2.884	3.520	3.546	5.360	7.013	3.462	6.959	5.606
09	-1.369	1.798	0.510	0.657	3.050	3.367	3.743	4.928	5.943	4.418	3.648	-1.408
10	-2.258	-0.631	-2.049	-1.440	0.149	-0.037	0.063	1.721	2.350	2.307	1.624	-1.304
11	-0.901	-1.369	-2.842	-2.317	-1.184	-1.017	-1.217	0.826	1.364	1.697	1.573	0.755
12	-0.334	-1.239	-2.800	-2.354	-1.292	-0.833	-1.239	0.850	1.461	1.792	1.897	1.569
13	0.764	-0.566	-2.215	-1.951	-0.997	0.293	-0.361	1.719	2.281	2.419	2.986	2.982
14	3.201	2.865	0.546	0.318	0.936	5.031	4.109	5.766	6.035	4.667	6.614	5.316
15	4.553	4.693	0.529	0.330	-0.282	4.000	2.550	4.027	4.774	3.493	6.021	5.786
16	4.710	4.817	0.529	0.334	-0.315	4.064	2.548	3.983	4.747	3.489	6.111	5.922
17	6.166	7.795	1.218	0.155	-1.463	4.341	2.603	4.041	4.791	2.946	7.506	8.864
18	-2.005	0.822	-0.600	-1.032	-7.342	-2.096	-3.100	-1.485	-1.417	-0.226	3.691	-0.633
19	-1.886	0.851	-0.585	-0.877	-7.217	-1.898	-2.985	-1.350	-1.312	-0.045	3.914	-0.607

trends, May shows highly significant increases at nearly all locations (often exceeding 3.8 cm yr^{-1}), highlighting a pronounced rise in stronger pre-monsoon waves. Strongly increasing trends during August confirm the intensification of energetic monsoon-driven wave conditions. Locations 15 & 16 in southern Kerala showed significant decrease of 0.8 cm yr^{-1} in near extreme SWH during March, suggesting localised reductions in near-extreme wave activity during transition months. Nevertheless, the overall signal across the coast is one of strengthening of both average and near-extreme wave heights, consistent with the observed increases in windspeed and supporting the conclusion that the dynamic wave climate along the Kerala coast is intensifying.

The monthly SHTS trends of both mean and near extreme (Tables 7 and 8), which predominantly reflect swell behaviour along the Kerala coast, show clear numerical coherence with the SWH trends during the pre-monsoon and monsoon

Table 4 Near-extreme monthly wind-speed trends (cm s^{-1} yr^{-1}) at the selected locations. Green shading indicates increasing trends, while red shading denotes decreasing trends, significant at 90% confidence level

Location	Jan	Feb	Mar	Apr	May	Jun	Jul	Aug	Sep	Oct	Nov	Dec
01	6.421	0.929	6.543	-0.450	10.314	6.893	-0.150	11.829	4.900	12.157	4.786	8.329
02	5.064	0.818	6.932	1.439	10.625	5.907	1.818	11.311	5.861	10.932	5.779	6.171
03	6.850	5.257	9.200	5.936	11.607	4.882	4.925	9.575	9.682	9.514	9.807	10.268
04	0.207	-0.346	2.254	1.554	6.754	-0.450	0.218	4.861	5.482	0.204	1.911	2.211
05	0.075	-1.525	2.775	2.129	7.596	0.639	2.175	7.754	6.214	0.411	1.421	3.789
06	8.211	8.743	4.100	1.986	7.686	1.754	4.329	5.507	6.900	1.082	9.218	5.811
07	8.346	9.886	3.650	1.989	7.925	2.168	4.632	6.886	6.579	2.271	9.014	6.029
08	7.168	10.846	-0.114	1.021	6.964	1.975	4.171	7.225	6.561	2.693	11.286	6.561
09	-1.279	1.850	0.786	1.196	6.950	0.579	5.571	8.911	6.646	5.471	4.200	-3.961
10	-3.232	-1.000	-3.432	-1.457	2.350	-3.943	1.079	5.575	1.721	2.879	0.304	-4.375
11	-2.511	-3.764	-5.554	-2.786	0.696	-3.936	-0.404	4.211	-0.296	2.064	0.375	-0.764
12	-2.696	-3.829	-5.900	-2.861	1.571	-3.821	0.086	4.218	0.157	2.161	0.654	0.714
13	-2.071	-2.304	-5.832	-1.804	3.096	-1.554	1.339	4.943	1.161	3.089	3.429	2.507
14	1.493	1.468	0.082	2.607	10.889	4.579	6.718	9.629	6.796	8.200	9.661	7.611
15	5.446	3.768	1.257	3.504	8.971	3.593	4.429	5.179	4.643	5.586	9.711	9.250
16	5.786	3.657	1.196	3.532	9.246	3.764	4.329	5.164	5.157	5.571	10.275	9.264
17	10.764	8.861	0.343	2.246	9.125	5.871	3.911	4.418	3.700	4.332	12.550	15.225
18	-1.593	-0.350	-2.307	-0.657	0.729	-3.254	-2.986	-1.918	-3.471	-2.411	5.846	-0.700
19	-1.368	-0.039	-2.061	-0.557	1.164	-3.461	-2.336	-1.836	-3.543	-1.814	5.761	-1.164

seasons. A prominent increase in mean SHTS occurs in May, where SHTS rises by 0.8–1.11 cm yr^{-1} across Locations 1–9, matching the corresponding SWH increases of 1.5–1.9 cm yr^{-1}, indicating that strengthening deep-water swell is directly amplifying nearshore wave heights. Similarly, during August, nearshore swell heights increase by 1.30–2.4 cm yr^{-1}, and SWH rises by 1.8–2.6 cm yr^{-1}, confirming that intensified monsoon-season swell energy is being transmitted shoreward. A comparable pattern in September, with SHTS increases of 0.65–0.80 cm yr^{-1}, aligns with SWH increases of roughly 0.8–1.04 cm yr^{-1}, further demonstrating the coupled deep-water and nearshore response to monsoon wave climate intensification.

While a few central locations (6–13) show weak negative trends in mean SHTS during March (−0.29 to −0.5 cm yr^{-1}), these are small in magnitude compared to the dominant positive trends during the energetic seasons. Overall, the concurrence of SHTS increases up to 2 cm yr^{-1} in

Table 5 Mean monthly significant wave height (SWH) trends (cm yr^{-1}) at the selected locations. Green shading indicates statistically significant increasing trends at the 90% confidence level

Location	Jan	Feb	Mar	Apr	May	Jun	Jul	Aug	Sep	Oct	Nov	Dec
01	0.573	-0.161	0.355	0.418	1.872	0.676	0.544	2.639	0.909	1.075	0.563	0.798
02	0.363	-0.290	0.119	0.169	1.604	0.593	0.453	2.481	0.774	0.785	0.417	0.556
03	0.486	-0.008	0.011	0.339	1.644	0.660	0.601	2.397	0.855	0.837	0.566	0.788
04	0.504	0.004	0.114	0.300	1.668	0.380	0.139	1.951	0.831	0.858	0.701	0.776
05	0.443	-0.100	0.098	0.197	1.637	0.652	0.531	2.252	0.982	0.859	0.697	0.725
06	0.313	-0.278	-0.059	-0.145	1.477	0.421	0.267	1.828	0.684	0.642	0.540	0.478
07	0.369	-0.254	-0.022	-0.137	1.609	0.491	0.286	1.956	0.772	0.692	0.607	0.553
08	0.275	-0.223	-0.186	-0.180	1.585	0.738	0.514	2.085	0.842	0.775	0.592	0.535
09	0.128	-0.304	-0.087	-0.046	1.574	0.707	0.555	1.912	0.895	0.866	0.636	0.442
10	0.088	-0.379	-0.100	-0.164	1.502	0.810	0.592	2.111	0.780	0.859	0.603	0.411
11	0.121	-0.355	-0.069	-0.148	1.469	0.837	0.627	1.971	0.760	0.903	0.625	0.440
12	0.121	-0.367	-0.069	-0.156	1.426	0.737	0.495	1.865	0.678	0.869	0.606	0.431
13	0.105	-0.350	-0.089	-0.174	1.405	0.943	0.747	2.069	0.749	0.868	0.530	0.381
14	0.189	0.012	-0.219	0.127	1.060	0.762	0.848	1.226	0.636	0.850	0.558	0.460
15	0.075	-0.137	-0.488	-0.108	1.271	0.514	0.054	1.357	0.603	0.885	0.420	0.343
16	0.078	-0.136	-0.488	-0.105	1.268	0.472	0.014	1.315	0.600	0.876	0.426	0.349
17	0.145	0.099	-0.296	0.122	1.617	1.723	1.418	2.282	1.041	0.952	0.624	0.528
18	0.041	0.046	-0.392	-0.063	1.273	1.152	0.533	1.594	0.830	0.773	0.488	0.382
19	0.027	0.038	-0.387	-0.086	1.296	1.198	0.514	1.783	0.954	0.768	0.463	0.358

May and nearly 4 cm yr^{-1} in August, combined with SWH increases of similar magnitude, confirms an overall rise in swell energy reaching the Kerala coast. This behaviour is consistent with the strengthened offshore wind forcing and deep-water SWH trends identified earlier, demonstrating that changes in the basin-scale wave climate are now manifesting as persistent increases in nearshore swell heights along the region.

The monthly trends of wind speed and wind-sea height (SHWW) show strong numerical coherence, confirming the tight coupling between atmospheric forcing and locally generated wave energy along the Kerala coast (Tables 3 and 9). The northern locations (1–3), which record the strongest mean wind-speed increases during the monsoon month August, with trends of +6.3 to +6.5 cm s^{-1} yr^{-1}, exhibit correspondingly high SHWW increases of +1.35 to +1.54 cm

Table 6 Near-extreme (90th percentile) monthly significant wave height (SWH) trends (cm yr^{-1}) at the selected locations. Green and red shading indicate statistically significant increasing and decreasing trends, respectively, at 90% confidence level

Location	Jan	Feb	Mar	Apr	May	Jun	Jul	Aug	Sep	Oct	Nov	Dec
01	1.203	-0.462	-0.010	0.738	4.178	1.998	0.702	3.628	0.185	1.990	-0.491	1.746
02	0.963	-0.739	-0.205	0.399	3.873	1.717	0.801	3.555	0.147	1.761	-0.563	1.476
03	1.113	-0.403	-0.199	0.567	3.867	1.405	0.853	3.366	0.451	1.361	-0.438	1.748
04	1.023	-0.521	0.205	0.514	3.822	0.961	0.194	3.001	0.252	1.246	-0.404	1.453
05	0.903	-0.668	0.250	0.323	3.880	1.531	0.715	3.476	0.478	1.277	-0.354	1.329
06	0.516	-0.890	0.217	0.222	3.767	0.760	1.024	3.177	0.262	1.101	-0.453	0.888
07	0.539	-0.918	0.296	0.202	4.095	0.767	1.053	3.434	0.361	1.213	-0.457	0.911
08	0.456	-0.927	-0.021	0.223	3.927	0.885	1.262	3.630	0.505	1.385	-0.479	0.795
09	0.320	-1.088	0.080	0.068	3.792	0.705	1.245	2.993	0.363	1.196	-0.274	0.911
10	0.277	-1.112	-0.041	-0.037	4.035	0.714	1.491	3.399	0.405	1.398	-0.330	0.830
11	0.209	-1.076	-0.067	-0.129	4.068	0.659	1.474	3.221	0.367	1.404	-0.096	0.763
12	0.160	-1.098	-0.062	-0.217	3.989	0.640	1.444	3.084	0.181	1.347	-0.062	0.732
13	0.108	-1.073	-0.059	-0.288	3.929	0.814	1.683	3.435	0.435	1.689	0.036	0.710
14	0.337	-0.561	-0.223	0.326	2.652	1.402	1.580	3.010	0.741	0.666	0.263	0.646
15	0.213	-0.892	-0.858	-0.057	3.800	1.197	0.480	2.434	0.622	1.169	-0.002	0.551
16	0.240	-0.897	-0.863	-0.049	3.838	1.117	0.454	2.355	0.653	1.115	0.012	0.525
17	0.289	-0.363	-0.301	0.184	4.287	2.629	2.523	3.957	1.291	1.161	0.587	0.761
18	-0.011	-0.185	-0.392	-0.064	3.933	2.135	1.157	2.750	0.835	0.750	0.570	0.468
19	-0.050	-0.208	-0.375	-0.063	4.040	1.910	0.901	2.684	1.008	1.051	0.557	0.425

yr^{-1} in the same period. Similarly, near-extreme winds at these locations rise by +9 to 12 cm s^{-1} yr^{-1} in August, matched by near-extreme SHWW increases of +1.9 to 2 cm yr^{-1}, indicating a clear amplification of high-energy wind-sea events during the monsoon peak (Table 10).

Eravipuram (Location 17) exhibits strong winter, and post-monsoon increases in mean wind speed (+6.16 cm s^{-1} yr^{-1} in January, +7.51 cm s^{-1} yr^{-1} in November, and +8.86 cm s^{-1} yr^{-1} in December). However, the corresponding SHWW trends remain weak, with mean SHWW increases of only +0.073, +0.675, and +0.339 cm yr^{-1} and near-extreme SHWW trends of +0.193, −0.058, and +0.744 cm yr^{-1} during these months. This indicates that, unlike during the monsoon season, strengthened northeasterly winter winds at this location do not result in increased wind-sea generation, highlighting the seasonal dependence of wind-sea response to wind forcing. In contrast, the southernmost stations (18 and 19) show significant negative wind-speed

Table 7 Mean monthly SHTS trends (cm yr^{-1}) at the selected locations. Green shading indicates statistically significant increasing trends, while red shading denotes statistically significant decreasing trends, at 90% confidence level

Location	Jan	Feb	Mar	Apr	May	Jun	Jul	Aug	Sep	Oct	Nov	Dec
01	0.307	0.205	-0.129	0.498	1.115	0.917	0.966	2.368	0.413	0.268	0.205	0.435
02	0.098	-0.002	-0.327	0.224	0.827	0.682	0.748	2.115	0.179	-0.026	0.000	0.188
03	0.301	0.222	-0.282	0.448	1.004	0.732	0.910	2.104	0.369	0.306	0.171	0.522
04	0.327	0.274	-0.129	0.461	1.068	0.482	0.450	1.734	0.454	0.406	0.227	0.542
05	0.252	0.195	-0.177	0.360	0.979	0.567	0.676	1.865	0.419	0.313	0.171	0.466
06	-0.031	-0.111	-0.446	-0.039	0.829	0.319	0.356	1.385	0.036	-0.116	-0.153	0.078
07	-0.020	-0.092	-0.438	-0.026	0.888	0.341	0.307	1.392	0.038	-0.115	-0.146	0.090
08	-0.020	-0.060	-0.576	-0.041	0.865	0.498	0.458	1.442	0.181	-0.019	-0.175	0.115
09	0.041	0.011	-0.377	0.141	1.019	0.490	0.576	1.378	0.451	0.170	0.014	0.244
10	-0.008	-0.042	-0.358	0.031	1.022	0.691	0.679	1.689	0.294	0.065	-0.069	0.148
11	-0.017	-0.060	-0.310	0.025	0.984	0.609	0.620	1.448	0.278	0.066	-0.084	0.140
12	-0.018	-0.068	-0.292	0.011	0.967	0.556	0.526	1.401	0.197	0.020	-0.106	0.128
13	-0.032	-0.095	-0.306	-0.042	0.937	0.714	0.703	1.594	0.172	-0.022	-0.193	0.093
14	0.227	0.249	-0.271	0.344	0.811	0.525	0.784	0.954	0.535	0.439	0.024	0.393
15	0.037	-0.015	-0.608	0.011	0.687	0.116	-0.045	0.853	0.354	0.265	-0.361	0.128
16	0.038	-0.011	-0.613	0.013	0.681	0.063	-0.100	0.802	0.365	0.267	-0.366	0.129
17	0.146	0.150	-0.389	0.249	1.161	1.281	1.437	1.986	0.801	0.375	-0.017	0.367
18	0.080	0.059	-0.413	0.110	0.817	0.600	0.538	1.260	0.680	0.279	-0.161	0.286
19	0.031	0.001	-0.465	0.035	0.776	0.583	0.463	1.364	0.714	0.221	-0.240	0.216

trends in January (−1.8 to −2 cm s^{-1} yr^{-1}) and a sharper decline in May (−7.2 to −7.3 cm s^{-1} yr^{-1}), paired with weak or negative SHWW responses of −0.013 to 0.020 cm yr^{-1} (mean) and 0.086 to 0.099 cm yr^{-1} (near-extreme) during January, confirming reduced wind-sea generation under weakening local winds.

One of the major climate modes which affects the weakening of winds in the north Indian ocean is SAM (Sreejith et al. 2023). Table S1 in supplementary material shows a negative correlation with SWH in May months especially in the southernmost locations. The influence of SAM may be one of the reasons for decreasing trend on wave and wind in the southernmost locations. These quantified patterns demonstrate that months with intensified wind forcing—particularly May, August and September—correspond to the largest SHWW increases (up to +1.50 cm yr^{-1} mean and +4.2 cm yr^{-1} near-extreme), whereas months with declining winds show negligible or negative wind-sea trends. Overall,

Table 8 Near-extreme monthly SHTS trends (cm yr^{-1}) at the selected locations. Green shading indicates statistically significant increasing trends, while red shading denotes statistically significant decreasing trends, at 90% confidence level

Location	Jan	Feb	Mar	Apr	May	Jun	Jul	Aug	Sep	Oct	Nov	Dec
01	0.548	-0.081	-0.630	0.862	1.610	1.596	1.683	3.737	0.559	0.421	0.286	0.977
02	0.198	-0.343	-0.750	0.535	1.309	1.400	1.579	3.647	0.394	-0.117	0.031	0.571
03	0.462	-0.190	-0.674	0.640	1.423	1.260	1.599	3.481	0.718	0.576	0.458	1.069
04	0.299	-0.059	-0.323	0.551	1.614	0.849	1.018	3.143	0.615	0.621	0.463	0.847
05	0.177	-0.064	-0.362	0.325	1.558	1.204	1.289	3.382	0.625	0.478	0.376	0.719
06	-0.160	-0.408	-0.698	-0.024	1.873	0.715	1.343	2.735	0.024	-0.123	-0.109	0.149
07	-0.118	-0.376	-0.754	0.038	2.143	0.597	1.308	2.834	0.012	-0.206	-0.130	0.187
08	-0.169	-0.475	-1.036	0.027	2.154	0.881	1.486	3.081	0.266	-0.061	-0.370	0.225
09	-0.141	-0.267	-0.435	0.398	1.911	0.731	1.286	2.540	0.633	0.426	0.167	0.272
10	-0.112	-0.206	-0.377	0.228	2.555	0.917	1.759	3.028	0.180	0.312	-0.001	0.220
11	-0.064	-0.276	-0.276	0.225	2.315	0.689	1.369	2.759	0.280	0.270	0.040	0.201
12	-0.050	-0.290	-0.285	0.172	2.338	0.662	1.353	2.604	0.131	0.193	0.079	0.159
13	-0.065	-0.293	-0.310	-0.088	2.502	0.984	1.724	2.925	0.118	0.235	-0.080	0.113
14	0.262	-0.116	-0.168	0.681	1.192	0.786	1.991	2.535	0.560	0.837	0.290	0.441
15	0.014	-0.561	-0.807	0.057	1.192	0.149	0.735	1.623	0.275	0.670	-0.388	0.127
16	-0.016	-0.555	-0.814	0.081	1.130	0.061	0.642	1.562	0.308	0.673	-0.337	0.114
17	0.137	-0.191	-0.348	0.588	2.334	1.991	2.764	3.996	1.154	0.829	0.186	0.398
18	-0.006	-0.111	-0.350	0.120	1.584	1.101	1.462	2.388	1.022	0.698	0.024	0.408
19	-0.038	-0.144	-0.394	0.015	1.585	0.861	1.154	2.262	1.073	0.658	-0.072	0.295

the results confirm that the observed SWH variability along the Kerala coast is strongly controlled by changes in local wind climate, with both the magnitude and seasonality of wind-sea trends closely mirroring mean and near-extreme wind-speed changes.

To further strengthen these model results, a few locations that are close to Kerala coast has been selected from ERA5 data for all wave parameters and monthly mean trends have been calculated (Table S2–S7). For SWH (Table S2, supplementary material), the northern locations show significant positive trend during August and negative trends are observed towards the southern locations. This agrees with our modelled monthly trend values and shows an increase in SWH during late monsoon periods along northern Kerala coast.

To understand the extreme wave activity at the selected 19 locations, the rough wave days index (Annual count of days when the daily SWH maximum is greater than

Table 9 Mean monthly SHWW trends (cm yr^{-1}) at the selected locations. Green shading indicates statistically significant increasing trends at 90% confidence level

Location	Jan	Feb	Mar	Apr	May	Jun	Jul	Aug	Sep	Oct	Nov	Dec
01	0.477	-0.368	0.518	0.055	1.505	0.191	-0.092	1.539	0.804	1.082	0.526	0.625
02	0.389	-0.369	0.386	-0.030	1.408	0.252	-0.050	1.505	0.782	0.959	0.509	0.542
03	0.376	-0.224	0.234	-0.059	1.274	0.275	-0.016	1.371	0.753	0.750	0.538	0.525
04	0.398	-0.216	0.223	-0.090	1.240	0.143	-0.205	1.129	0.665	0.698	0.649	0.520
05	0.394	-0.266	0.236	-0.115	1.278	0.413	0.120	1.426	0.860	0.772	0.682	0.527
06	0.378	-0.265	0.182	-0.163	1.210	0.330	0.045	1.262	0.718	0.757	0.653	0.502
07	0.420	-0.250	0.201	-0.152	1.328	0.404	0.107	1.418	0.808	0.796	0.705	0.566
08	0.344	-0.227	0.162	-0.176	1.282	0.582	0.268	1.508	0.842	0.849	0.720	0.544
09	0.184	-0.350	0.160	-0.186	1.177	0.540	0.234	1.358	0.745	0.864	0.674	0.397
10	0.154	-0.380	0.113	-0.218	1.130	0.547	0.196	1.387	0.725	0.897	0.666	0.414
11	0.179	-0.341	0.112	-0.186	1.125	0.645	0.310	1.412	0.705	0.939	0.696	0.440
12	0.176	-0.346	0.101	-0.187	1.090	0.565	0.216	1.314	0.657	0.921	0.683	0.433
13	0.159	-0.321	0.089	-0.168	1.079	0.710	0.387	1.413	0.753	0.941	0.647	0.390
14	0.070	-0.198	-0.048	-0.187	0.587	0.581	0.442	0.795	0.375	0.646	0.559	0.230
15	0.082	-0.143	-0.118	-0.150	0.960	0.564	0.067	1.048	0.475	0.806	0.662	0.314
16	0.082	-0.145	-0.113	-0.149	0.957	0.549	0.056	1.034	0.461	0.793	0.669	0.319
17	0.073	-0.005	-0.036	-0.087	1.039	1.183	0.551	1.275	0.685	0.830	0.675	0.339
18	-0.013	0.017	-0.150	-0.210	0.847	1.007	0.216	1.034	0.518	0.694	0.617	0.228
19	0.020	0.066	-0.085	-0.155	0.916	1.076	0.256	1.196	0.644	0.730	0.655	0.264

2.5 m) given by the joint CCI/WCRP-CLIVAR/JCOMM Expert Team on Climate Change Detection and Indices (ETCCDI) (WCRP, 2020) is also analysed using a heat-map (Fig. 5).

A clear spatial gradient emerges, with the northern Kerala locations (1–3) consistently showing the highest counts (mostly > 15 days/yr), whereas southern locations (14–19) are mostly near zero or single digits except in recent years. Locations 4 and 16 have low annual counts throughout 2007–2017, while sites 17–19 often had zero or a few days in the same period. Importantly, 2018 stands out as an extreme anomaly, during which all locations from 1 to 8 shows a large increase in rough-wave days that year (with values up to 43 and 41 at northern locations 1 and 2, compared to earlier counts of ~25). Many central locations (4–8) also jump from ~0–7 days in other

Table 10 Near-extreme monthly SHWW trends (cm yr^{-1}) at the selected locations. Green shading indicates statistically significant increasing trends at 90% confidence level

Location	Jan	Feb	Mar	Apr	May	Jun	Jul	Aug	Sep	Oct	Nov	Dec
01	0.760	-0.723	1.045	0.046	3.791	0.954	-0.048	2.000	0.261	2.501	-0.777	1.344
02	0.590	-0.807	0.809	0.019	3.569	0.932	0.011	2.069	0.117	2.366	-0.762	1.305
03	0.644	-0.658	0.641	0.181	3.228	0.920	0.129	1.998	0.155	1.849	-0.760	1.245
04	0.624	-0.703	0.630	0.179	3.189	0.598	-0.197	1.807	0.071	1.251	-0.621	1.181
05	0.612	-0.767	0.650	0.255	3.385	0.822	0.189	2.333	0.346	1.411	-0.537	1.114
06	0.457	-0.815	0.545	0.189	3.142	0.530	0.434	2.381	0.139	1.160	-0.373	0.827
07	0.441	-0.886	0.620	0.188	3.445	0.675	0.494	2.650	0.273	1.265	-0.406	0.826
08	0.339	-0.786	0.375	0.040	3.318	0.668	0.687	2.655	0.340	1.426	-0.350	0.763
09	0.294	-0.967	0.189	-0.114	3.375	0.519	0.859	2.379	0.200	1.359	-0.413	0.702
10	0.236	-1.098	0.057	-0.194	3.508	0.540	0.770	2.516	0.231	1.465	-0.297	0.729
11	0.164	-1.101	0.036	-0.208	3.675	0.584	0.994	2.565	0.241	1.541	-0.154	0.666
12	0.143	-1.100	-0.005	-0.226	3.608	0.517	0.899	2.408	0.126	1.463	-0.110	0.653
13	0.147	-1.051	-0.030	-0.229	3.557	0.693	1.061	2.575	0.340	1.675	0.045	0.640
14	0.173	-0.635	-0.141	-0.416	2.418	1.045	1.064	1.960	0.568	0.931	-0.131	0.396
15	0.240	-0.608	-0.339	-0.573	3.797	1.112	0.605	2.191	0.393	1.321	-0.106	0.491
16	0.225	-0.642	-0.255	-0.558	3.807	1.098	0.615	2.191	0.424	1.264	-0.097	0.472
17	0.193	-0.311	-0.200	-0.521	3.892	1.945	1.123	2.271	0.851	1.296	-0.058	0.744
18	0.086	-0.173	-0.503	-0.749	4.169	1.651	0.775	2.039	0.698	1.139	0.031	0.601
19	0.099	-0.131	-0.401	-0.652	4.223	1.574	0.734	2.085	0.872	1.340	0.138	0.571

years to double-digit counts (e.g. 17 days at site 07, 13 at location 8). Post-2018 (2019–2021), most locations have a low number of rough wave days (though some northern sites remain modestly elevated). Southern sites (17–19) which had zero through 2017, show slight increases after 2018 (e.g. up to 5–6 days by 2020–21). Overall analysis shows the rough wave days are more in northern Kerala. It also indicates 2018 as an anomalous year which has to be explored further.

3.2 Spatial trend analysis in the Indian Ocean

Previous studies, such as Chowdhury et al. (2019), have posited that the rise in wave heights along the Indian coast is driven by an increase in swells originating from the Southern Ocean and subsequently propagating into the NIO. Some earlier studies have documented this propagation of long-distance swell from the Southern Ocean to the Indian Ocean (Young 1999; Zheng et al. 2018). To identify

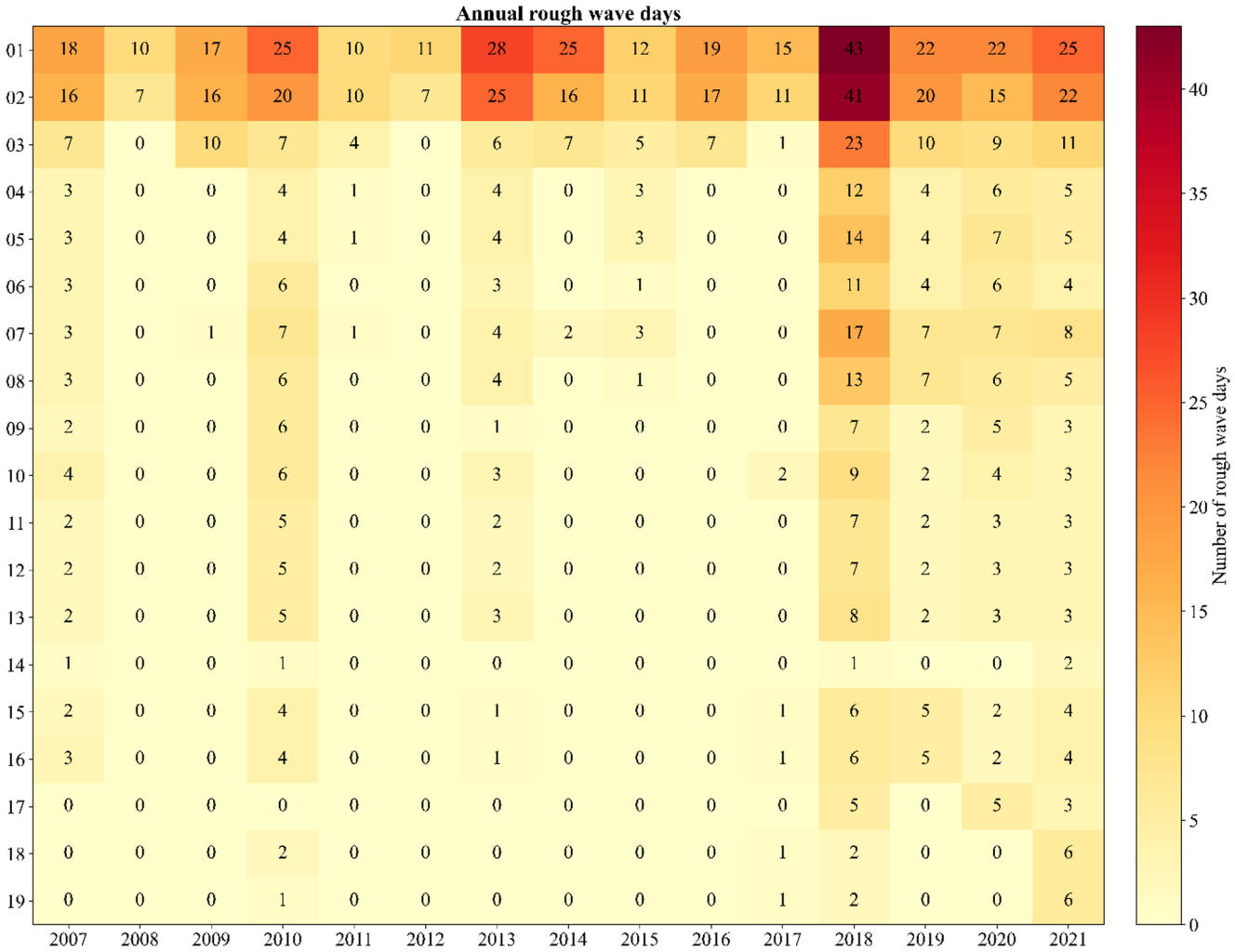

Fig. 5 Heatmap of rough wave days at selected 19 locations along Kerala coast from 2007–2021

the observed trends and to explore its potential link with the Southern Ocean, we conducted a spatial trend analysis of SWH, SHTS and SHWW. Positive SWH trends (Fig. 6) are prominent in the southern Indian Ocean (~40°S–60°S) from May to September, except august corresponding to the austral winter. Positive trends are prominent in the southwest coast of India during May and August in the spatial trend analysis of NIO. The spatial positive trend seen during the month of august is mostly in the NIO with the highest values in the AS. Whereas the positive trend observed in the SWH during May can be linked to Southern Ocean. The positive trends in May and August is in agreement with the significant trends observed for the locations as per our earlier analysis. The analysis of SHTS (Fig. 7) supports the positive trend observed in May and its linkage to swells originating from the Southern Ocean. In contrast, the positive SHTS trend during August, confined to the northern Indian Ocean (NIO), indicates variations associated with monsoon-generated swells. Strong negative trends are seen in the southern Indian Ocean (especially around 40°S–60°S) during the first half of the year, with mild positive trends re-emerging from June to September, aligned with swell propagation from the Southern Ocean. These results agree with the study of Erikson et al. (2022). The SHWW trends are seen significant in the NIO during the month May and August. It is an indication of the contribution of SHTS and SHWW to the positive trend of SWH in NIO.

During May to September months, SWH and SHWW (Fig. 8) increase significantly in the Arabian Sea and western Bay of Bengal, indicative of intensified southwest monsoon waves. SHTS shows significant positive trends in the NIO during the months May, August, and September.

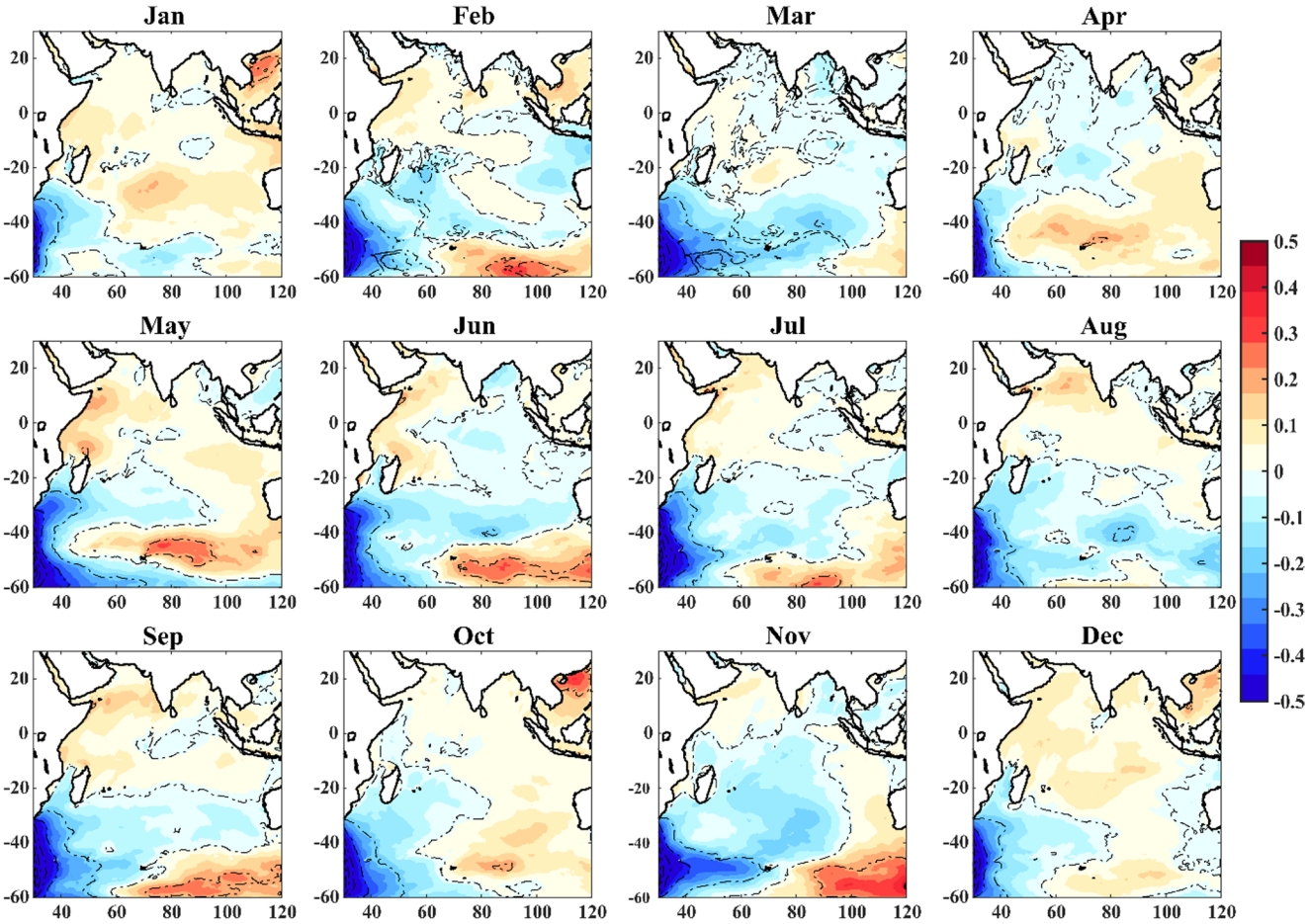

Fig. 6 Spatial trend of near-extreme (90th percentile) significant wave height (SWH). Contours represent 90% significance

4 Summary and conclusion

The present study analysed wave climate variability over a 15-year period (2007–2021) across 19 erosion and inundation hotspots along the Kerala coast using WAVEWATCH III simulations and ERA5 reanalysis. The focus was on trends in significant wave height (SWH), swell wave height (SHTS), and wind-sea height (SHWW), validated using buoy data. Results revealed clear spatial and temporal patterns, with the northernmost location, Musodi Beach, showing the highest trend in annual mean SWH, while Eravipuram in the south recorded the highest trend in annual near-extreme SWH. Statistically significant increases were especially evident during May and August, months linked with intensified monsoonal forcing and remote swell propagation. A maximum upward trend in monthly mean SWH of 2.639 cm/year was recorded at the northernmost location, Musodi beach during August. A significant upward trend in near-extreme SWH ranging from 2.5 to 4 cm/year was observed during May and August with the highest upward trend of 4.287 cm/year recorded at Eravipuram.

Separate trend analysis of significant wave height of total swell (SHTS) and wind sea (SHWW) was carried out. Monthly trend analysis of SHTS and SHWW also exhibited a significant upward trend in May and August months at most of the locations. The observed trends in SWH, SHTS and SHWW were cross referenced with ERA5 data for the same period revealing a close alignment with each other which confirms the reliability of the results (Tables S2–S7 are provided in the supplementary material).

The results clearly demonstrate that the wave climate along the Kerala coastline is undergoing a measurable intensification, driven predominantly by changes in regional wind forcing and the strengthening of Indian Ocean swell systems. The northern hotspots show the strongest increases in both wind-sea and total SWH, highlighting their sensitivity to a more energetic monsoon wind field. In contrast, the southernmost locations exhibit declining wind trends and correspondingly weak wind-sea and wave responses, indicating a spatial gradient in climatic influence along the coast. A possible cause is the recent increase in monsoon depressions over the North Arabian Sea and the poleward

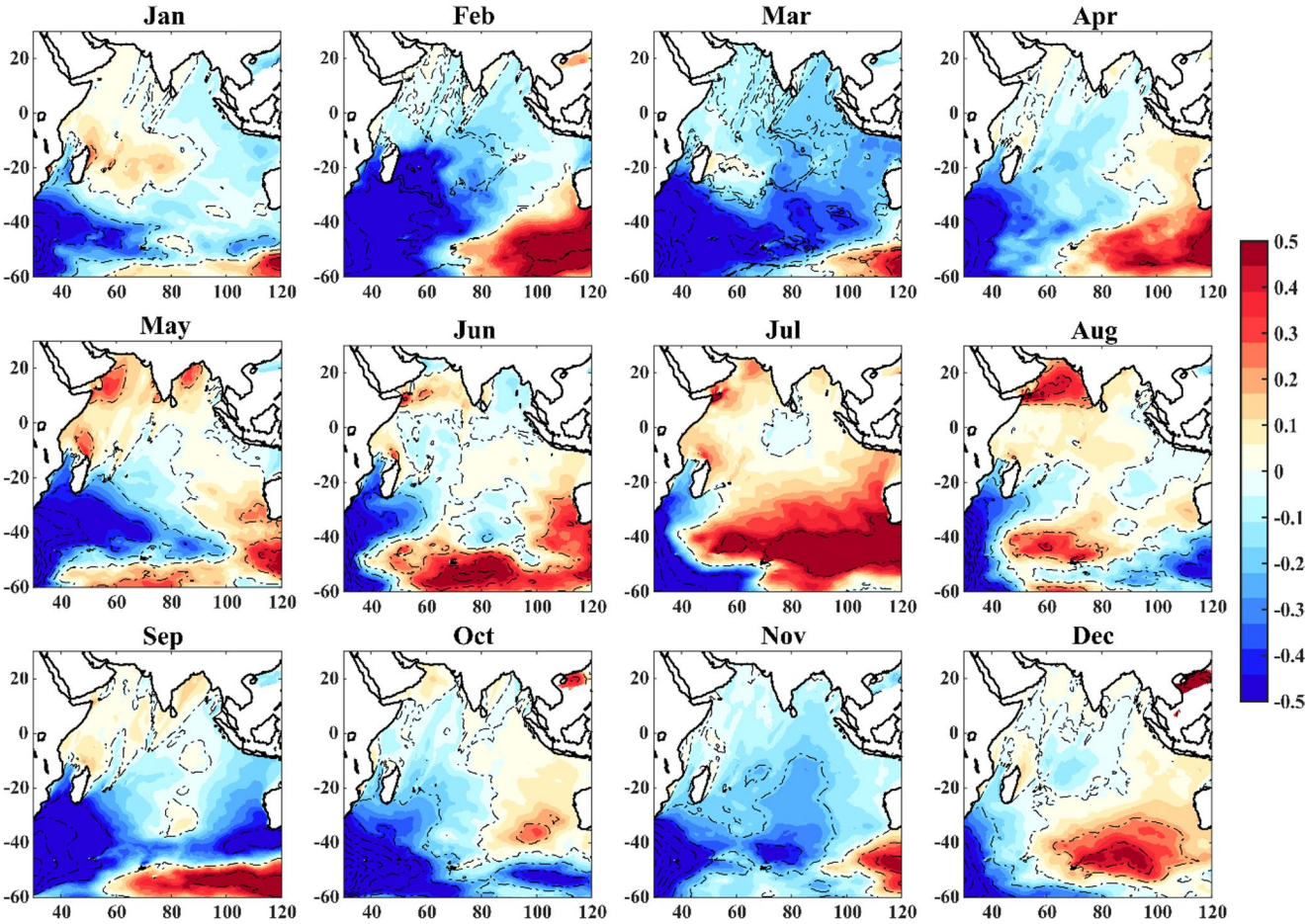

Fig. 7 Spatial trend of near-extreme (90th percentile) significant wave height of total Swell (SHTS). Contours represent 90% significance

shift of the monsoon low-level jet, which strengthen southwesterly winds and monsoon pulses over the northern Arabian Sea, enhancing wind and wave activity along northern Kerala (Chilukoti et al. 2024).

The consistent rise in SWH and SHTS in conjunction with increasing wind-sea height confirms that both local wind forcing and remote swell propagation are contributing to higher nearshore wave energy. These changes have important implications for coastal erosion, sediment mobility, and shoreline management along the Kerala coast, particularly at vulnerable hotspots. The findings emphasize the need for continuous wave-climate monitoring and incorporation of evolving wave trends into coastal planning frameworks to mitigate future risks.

A significant finding was the sharp upward trends in both mean and near-extreme wave parameters during the months of May and August. These trends were consistent across multiple locations and wave types—indicating a systemic shift in the regional wave climate. The alignment of model-based trends with ERA5 data lends further confidence to the robustness of these results. Spatial trend analyses further revealed a steady increase in wave height in the Southern Ocean during these months, confirming the distant influence of Southern Ocean swell systems on the Kerala coast.

These results are consistent with the findings of Sreejith et al. (2023) who highlighted the influence of the Southern Annular Mode (SAM) on Indian Ocean wave dynamics. Positive phases of SAM intensify the Southern Ocean westerlies, enhancing swell generation, also shift the swell generation area and more swell propagation towards Arabian Sea and which can be clearly seen in the spatial trend of SHTS during May. The significant increases in SHTS during May and August corroborate this linkage, suggesting that the increasing wave energy along the Kerala coast is not solely a result of local forcing but also influenced by far-field climate variability such as SAM. This confirms the existence of a teleconnection between mid-latitude atmospheric circulation and tropical coastal wave regimes. Also, the study of Remya et al. (2020) shows that the positive SAM and ENSO exacerbate positive trend of SWHin the southwest coast of India.

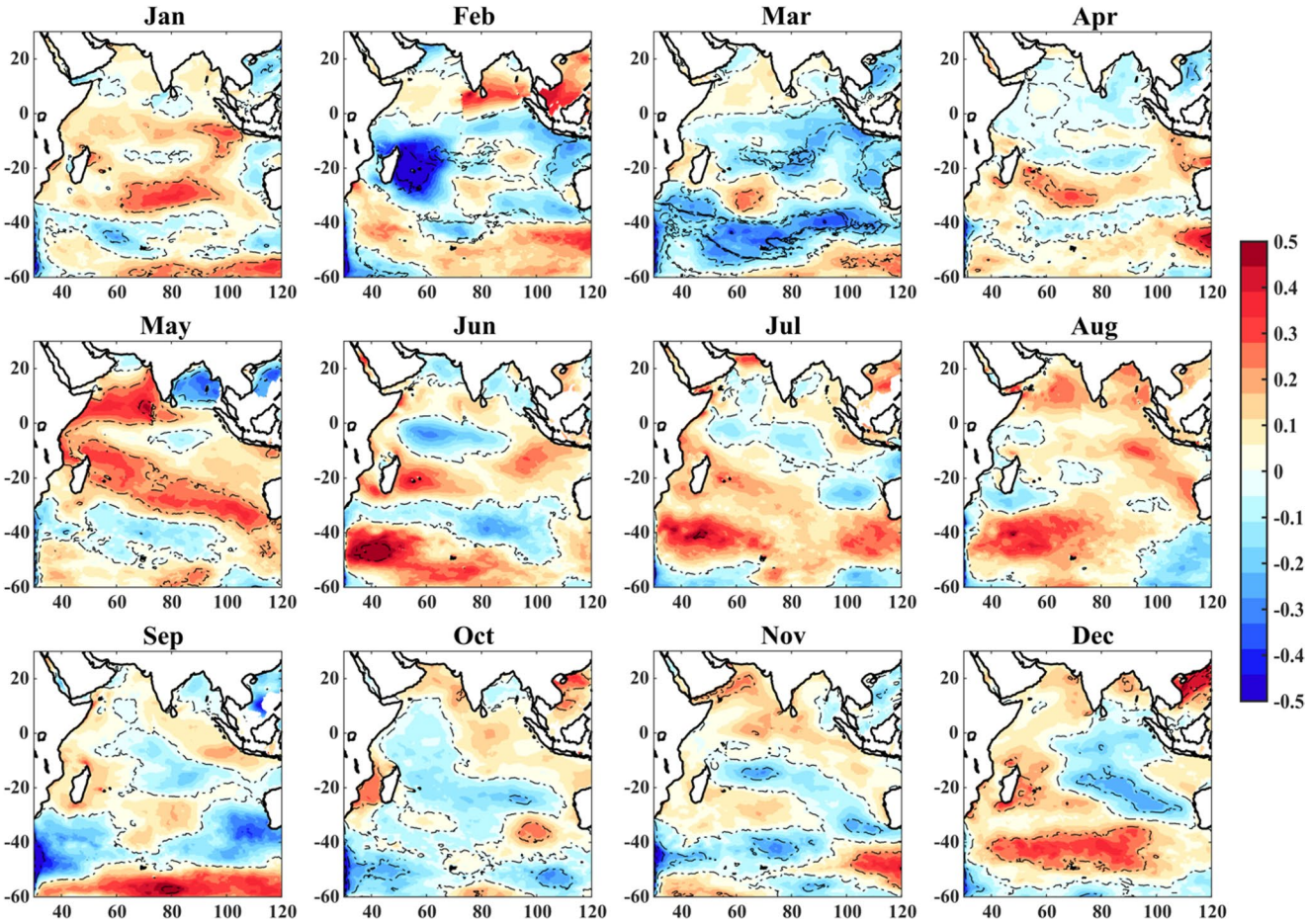

Fig. 8 Spatial trend of near-extreme (90th percentile) significant wave height of wind sea (SHWW). Contours represent 90% significance

The broader implications of this work are significant. Rising wave energy, particularly from increased swell dominance, poses challenges for shoreline stability, infrastructure safety, and disaster preparedness. These findings emphasize the urgency of integrating wave climate trends into long-term coastal zone management. The study provides compelling evidence that remote climate drivers are amplifying regional wave climate variability.

In the context of climate change, the results point to a future where intensified Southern Ocean storm systems, linked to global warming and poleward-shifting westerlies, will continue to elevate swell energy reaching the Indian Ocean. The Kerala coast, due to its geographic orientation and exposure, is particularly sensitive to such changes. Therefore, sustained wave climate monitoring and adaptive planning are crucial to mitigate the compounding risks of climate-driven coastal hazards.

Supplementary Information The online version contains supplementary material available at https://doi.org/10.1007/s10236-026-01786-8.

Acknowledgements This research falls under OCCAS-Deep Ocean Mission(DOM), MoES, Govt. India. We thank the developers of WAVEWATCH III NOAA/NCEP for providing the WAVEWATCH III source code (https://polar.ncep.noaa.gov/waves/) and for their consistent efforts to improve the accuracy of this open-source spectral model.The authors would like to thank Dr. Sekhar Lukose Kuriakose, Member Secretary, KSDMA for his support. Authors also thank the Observation, Data management and ICT divisions of INCOIS for their support. The wave model experiments are performed in MIHIR HPC. The first and fourth authors would like to acknowledge the National Centre for Coastal Research (NCCR), India for the financial support funded through the project MoES/NCCR/CP&SM/GIA-KUFOS/3/2022. This is INCOIS contribution no. 700.

Author contributions PA: Software, Methodology, Formal analysis, Writing – Original draft, PGR: Writing – Original draft, Methodology, Conceptualization, Formal analysis, MS: Data curation, Formal analysis, Writing – Original draft. PS: Writing – review & editing. RR: Writing – review & editing, BPK: Writing – review & editing, AJ: Data curation TMB: Writing – review & editing.

Data availability No datasets were generated or analysed during the current study.

Declarations

Competing interests The authors declare no competing interests.

References

Abdulla CP, Aboobacker VM, Shanas PR, Vijith V, Sajeev R, Vethamony P (2022) Climatology and variability of wind speeds along the southwest coast of India derived from Climate Forecast System Reanalysis winds. Int J Climatol 42(16):8738–8754

Abdulla CP, Aboobacker VM, Vethamony P (2023) Climate, trends and variability of extreme winds along the southwest coast of India. Int J Climatol 43(16):7775–7794

Almar R, Kestenare E, Reyns J, Jouanno J, Anthony EJ, Laibi R, Hemer M, Du Penhoat Y, Ranasinghe R (2015) Response of the Bight of Benin (Gulf of Guinea, West Africa) coastline to anthropogenic and natural forcing, Part1: Wave climate variability and impacts on the longshore sediment transport. Cont Shelf Res 110:48–59

Ananthu P, Shanas PR, Komath S et al (2026) Wave climate of Kerala Coast: An 83-Year ERA-5 study of trends and seasonality. Earth Syst Environ 10:117–138. https://doi.org/10.1007/s41748-024-00561-3

Ardhuin F, Rogers E, Babanin AV, Filipot JF, Magne R, Roland A, Van Der Westhuysen A, Queffeulou P, Lefevre JM, Aouf L, Collard F (2010) Semiempirical dissipation source functions for ocean waves. Part I: Definition, calibration, and validation. J Phys Oceanogr 40(9):1917–1941

Balakrishnan Nair TM, Anoop TR, Nherakkol A, Sanil Kumar V, Remya PG, Sandhya KG, Shesu V, Harikumar R, Jeyakumar R, Singh C, J. and, Majumdar S (2025) WAve Monitoring Along Nearshore (WAMAN) Buoy Network: Best practices and applications in sea state monitoring and forecasting for the Indian Ocean. Bull Am Meteorol Soc 106(11):E2196–E2212

Beaven RP, Stringfellow AM, Nicholls RJ, Haigh ID, Kebede AS, Watts J (2020) Future challenges of coastal landfills exacerbated by sea level rise. Waste Manag 105:92–101

Chawla A et al (2007) A multigrid wave forecasting model: A new paradigm in operational wave forecasting. Weather Forecast 28:1057–1078. https://doi.org/10.1175/WAF-D-12-00007.1

Chilukoti N, Nimmakanti M, Chowdary JS (2024) Recent two decades witness an uptick in monsoon depressions over the northern Arabian Sea. npj Clim Atmos Sci 7:183. https://doi.org/10.1038/s41612-024-00727-w

Chowdhury P, Behera MR, Reeve DE (2019) Wave climate projections along the Indian coast. Int J Climatol 39(11):4531–4542

Erikson L, Morim J, Hemer M, Young I, Wang XL, Mentaschi L, Mori N, Semedo A, Stopa J, Grigorieva V, Gulev S (2022) Global ocean wave fields show consistent regional trends between 1980 and 2014 in a multi-product ensemble. Commun Earth Environ 3(1):320

Hameed TS (1988) Wave climatology and littoral processes at Alleppey. Ocean waves and beach processes of the southwest coast of India and their predictions. Centre Earth Sci Stud 67–90

Harish CM (1988) Waves and related nearshore processes in a complex bay beach at Tellicherry. Ocean waves and beach processes 183–204

Hersbach H, Bell B, Berrisford P, Hirahara S, Horányi A, Muñoz-Sabater J, Nicolas J, Peubey C, Radu R, Schepers D, Simmons A (2020) The ERA5 global reanalysis. Q J R Meteorol Soc 146(730):1999–2049

Kumar P, Kaur S, Weller E, Min SK (2019) Influence of natural climate variability on the extreme ocean surface wave heights over the Indian Ocean. J Geophys Research: Oceans 124(8):6176–6199

Kurian NP (1988) Waves and littoral processes at Calicut. Ocean Waves and Beach Processes of South West Coast of India and Their Prediction. Centre for Earth Science Studies, Trivandrum, India, pp 91–110

Kurian NP, Rajith K, Shahul Hameed TS, Sheela Nair L, Ramana Murthy MV, Arjun S, Shamji VR (2009) Wind waves and sediment transport regime off the south-central Kerala coast, India. Nat Hazards 49:325–345

Lemos G, Menendez M, Semedo A, Miranda PM, Hemer M (2021) On the decreases in North Atlantic significant wave heights from climate projections. Clim Dyn 57(9):2301–2324

Li J, Pan S, Chen Y, Fan YM, Pan Y (2018) Numerical estimation of extreme waves and surges over the northwest Pacific Ocean. Ocean Eng 153:225–241

Naseef TM, Kumar VS (2017) Variations in return value estimate of ocean surface waves–a study based on measured buoy data and ERA-Interim reanalysis data. Nat Hazards Earth Syst Sci 17:1763. https://doi.org/10.5194/nhess-17-1763-2017

Noujas V, Kurian NP, Thomas KV (2019) Comparison of coastal hydrodynamics in different energy regime coasts along southwest coast of India. J Earth Syst Sci 128:1–24

Ramakrishnan R, Remya PG, Mandal A, Mohanty P, Arayakandy P, Mahendra RS, Nair TB (2022) Wave induced coastal flooding along the southwest coast of India during tropical cyclone Tauktae. Sci Rep 12(1):19966

Remya PG, Vishnu S, Praveen Kumar B, Nair B, T.M. and, Rohith B (2016) Teleconnection between the N orth I ndian O cean high swell events and meteorological conditions over the S outhern I ndian O cean. J Geophys Research: Oceans 121(10):7476–7494

Remya PG, Kumar BP, Srinivas G, Balakrishnan Nair TM (2020) Impact of tropical and extra tropical climate variability on Indian Ocean surface waves. Clim Dyn 54:4919–4933. https://doi.org/10.1007/s00382-020-05262-x

Sabique L, Annapurnaiah K, Nair TB, Srinivas K (2012) Contribution of Southern Indian Ocean swells on the wave heights in the Northern Indian Ocean—A modeling study. Ocean Eng 43:113–120

SanilKumar V, Jesbin G (2016) Influence of Indian summer monsoon variability on the surface waves in the coastal regions of eastern Arabian Sea. Ann Geophys 34:871–885. https://doi.org/10.5194/angeo-34-871-2016

Saprykina Yana V, Samiksha SV, Yu KS (2021), Wave Climate variability and occurrence of mudbanks along the Southwest Coast of India. Front Mar Sci https://doi.org/10.3389/fmars.2021.671379

Shahul Hameed TS, Kurian NP, Thomas KV, Rajith K, Prakash TN (2007) Wave and current regime off the southwest coast of India. J Coastal Res 23(5):1167–1174

Shamji VR, Shahul Hameed TS, Kurian NP, Thomas KV (2010) Application of numerical modelling for morphological changes in a high-energy beach during the south-west monsoon. Curr Sci 98(5):691–695

Shanas PR, SanilKumar V (2014) Temporal variations in the wind and wave climate at a location in the eastern Arabian Sea based on ERA-Interim reanalysis data. Nat Hazards Earth Syst Sci 14:1371–1381. https://doi.org/10.5194/nhess-14-1371-2014

Sreejith M, Remya PG, Praveen Kumar B, Srinivas G, Balakrishnan Nair TM (2023) Impact of Southern Annular Mode on the Indian Ocean Surface Waves. Int J Climatol 43:16: 7606–7617. https://doi.org/10.1002/joc.8282

Sreelakshmi S, Bhaskaran PK (2020a) Regional wise characteristic study of significant wave height for the Indian Ocean. Clim Dyn 54(7–8):3405–3423

Sreelakshmi S, Bhaskaran PK (2020b) Spatio-temporal distribution and variability of high threshold wind speed and significant wave height for the Indian Ocean. Pure appl Geophys 177:4559–4575

Sreelakshmi S, Bhaskaran PK (2020c) Wind-generated wave climate variability in the Indian Ocean using ERA-5 dataset. Ocean Eng 209:107486

Sreelakshmi S, Bhaskaran PK (2023) Swell wave propagation and its characteristics while approaching the Indian Coast. Clim Dyn 60(5):1271–1295

Thomas KV (1988) Waves and nearshore processes in relation to beach development at Valiathura. Ocean waves and beach processes of south west coast of India and their prediction. Centre for Earth Science Studies, Trivandrum, pp 47–66

WCRP (2020) World Climate Research Programme, Expert Team on Climate Change Detection. https://www.wcrp-climate.org/data-etccdi

Young IR (1999) Wind generated ocean waves, vol 2. Elsevier

Young IR, Zieger S, Babanin AV (2011) Global trends in wind speed and wave height. Science 332(6028):451–455

Zheng CW, Li CY, Pan J (2018) Propagation Route and Speed of Swell in the Indian Ocean. J Geophys Res Oceans 123:8–21. https://doi.org/10.1002/2016JC012585